

## Effects of Cocooning on Coronavirus Disease Rates after Relaxing Social Distancing

Xutong Wang, Zhanwei Du, George Huang, Remy F. Pasco, Spencer J. Fox, Alison P. Galvani, Michael Pignone, S. Claiborne Johnston, Lauren Ancel Meyers

Author affiliations: The University of Texas at Austin, Austin, Texas, USA (X. Wang, Z. Du, G. Huang, R.F. Pasco, S.J. Fox, L.A. Meyers); Yale School of Public Health, New Haven, Connecticut, USA (A.P. Galvani); The University of Texas at Austin Dell Medical School, Austin (M. Pignone, S. Claiborne Johnston); Santa Fe Institute, Santa Fe, New Mexico, USA (L. Ancel Meyers)

DOI: <https://doi.org/10.3201/eid2612.201930>

As coronavirus disease spreads throughout the United States, policymakers are contemplating reinstatement and relaxation of shelter-in-place orders. By using a model capturing high-risk populations and transmission rates estimated from hospitalization data, we found that postponing relaxation will only delay future disease waves. Cocooning vulnerable populations can prevent overwhelming medical surges.

In March 2020, cities and states throughout the United States issued social distancing orders to mitigate the coronavirus disease (COVID-19) pandemic (1). In response to growing political and economic pressures, the White House and the Centers for Disease Control and Prevention issued guidelines for relaxing such measures on April 16, 2020 (2). However, the gating criteria in these guidelines do not include provisions, such as cocooning, to protect vulnerable populations. Residents of long-term care facilities (LTCFs) are particularly vulnerable because of congregate living, shortages in qualified workers, and the need for physical contact between caregivers and residents. In LTCFs, cocooning includes measures to increase staff; cohort residents; test for severe acute respiratory syndrome 2 (SARS-CoV-2), the causative agent of COVID-19; and assess availability of personal protective equipment and other infection control resources (3). Among other groups, cocooning involves incentivizing persons with high-risk underlying conditions to remain at home, helping persons experiencing homelessness to social distance, and broadly encouraging hand hygiene and wearing face masks for persons at high risk for severe illness or death and their caregivers (4).

By June 16, 2020, nursing home residents constituted 42.8% (50,919/119,055) of US COVID-19 deaths (5). In Austin, Texas, patients in LTCFs represented approximately half the COVID-19 deaths and  $\geq 20\%$  (81/398) of COVID-19 hospitalizations among persons with known residence (6).

To quantify the need for proactively protecting these vulnerable populations, we projected the effects of relaxation of shelter-in-place orders, with and without additional cocooning measures. We built a granular mathematical model of COVID-19 spread in US cities that incorporates age-specific and risk-stratified heterogeneity in the transmission and severity of COVID-19 (Appendix, <https://wwwnc.cdc.gov/EID/article/26/12/20-1930-App.pdf>) (7). The model uses 70 stochastic differential equations to track the disease status in 10 subpopulations: low-risk and high-risk persons in each of 5 age groups, 0–4 years, 5–17 years, 18–49 years, 50–64 years, and >64 years of age. We focused on the Austin-Round Rock Metropolitan Statistical Area in Texas, the fastest-growing large city area in the United States, because we provide decision support for city leaders and have access to patient-level COVID-19 hospitalization and death data.

Persons initially are susceptible to SARS-CoV-2 and infection rates are dependent on age-specific contact rates and prevalence of infection. Upon infection, persons incubate SARS-CoV-2 asymptomatically before progressing to a symptomatic or asymptomatic infectious state. Depending on age and risk group, symptomatic COVID-19 case-patients might be hospitalized and die. To model cocooning of high-risk populations, we reduced the transmission rate to and from persons >64 years of age and in younger high-risk subgroups.

Social distancing began in Austin with school closures on March 14, 2020 and ramped up on March 24, 2020 with a Stay Home–Work Safe order (order 20200324-007; <https://www.austintexas.gov>). We assumed published values for most model parameters (Table; Appendix) and calibrated the transmission rate before and after the stay-home order based on hospitalization counts (Figure). During March 24–April 23, data suggest that SARS-CoV-2 transmission dropped by 70% (95% CI 45%–100%). If social distancing measures were completely relaxed on May 1, 2020, we estimated that COVID-19 hospitalizations would surpass Austin's surge capacity of 3,440 beds in 27 (95% CI 16–43) days, on May 28 (Figure). Assuming instead that individual behavior and public health efforts continued to reduce transmission by 75% relative to

**Table.** Key parameters of a transmission model for coronavirus disease, Austin, Texas, USA\*

Parameter	Value				
Incubation period, d (range)	2.9 (1.9–3.9)				
Infectious period, d (range)	6.3 (5.3–7.3)				
Asymptomatic proportion, %	43				
Average hospitalization, d					
Recovered	10.96				
Died	8.2				
Transmission reduction during Stay Home–Work Safe Order, % (95% CI)†	70 (45%–100%)				
Cocooning efficacy, % reduction in transmission relative to Stay–Home Work Safe Order‡					
Cocooning	100				
Enhanced cocooning	125				
Age group, y	0–4	5–17	18–49	50–64	≥65
Symptomatic case hospitalization rate, %§					
Low-risk group	0.0279	0.0215	1.3215	2.8563	3.3873
High-risk group	0.2791	0.2146	13.2154	28.5634	33.8733
Infected fatality rate, %‡					
Low-risk group	0.0009	0.0022	0.0339	0.2520	0.6440
High-risk group	0.0092	0.0218	0.3388	2.5197	6.4402

\*Detailed parameter distributions and references are given in Appendix Tables 3, 4 (<https://wwwnc.cdc.gov/EID/article/26/12/20-1930-App.pdf>).

†Estimated by fitting the model to coronavirus disease hospitalization counts March 13–April 23.

‡The Appendix provides sensitivity analyses with respect to 2 key assumptions of the model: age-specific contact patterns, which might have changed during the recent unprecedented social distancing; and equally effective cocooning of persons at high risk across all age groups. Cocooning and enhanced cocooning are for persons ≥65 years of age and persons <65 years of age with high-risk underlying conditions.

§The hospitalization rate and fatality rate for the high-risk group is assumed to be 10 times higher than the corresponding low-risk group in the same age range. The overall hospitalization rate and fatality rate is based on the age-specific values listed in corresponding literature.

the stay-home order, hospital surge capacity would be reached after 84 (95% CI 41–137) days, on July 24. When we superimposed cocooning to reduce transmission risk by 125% relative to the stay-home

period for 547,474 persons at high risk among the total population of 2,168,316 (Appendix), Austin could avoid hospital surge and reduce cumulative COVID-19 hospitalizations by 62% and deaths by

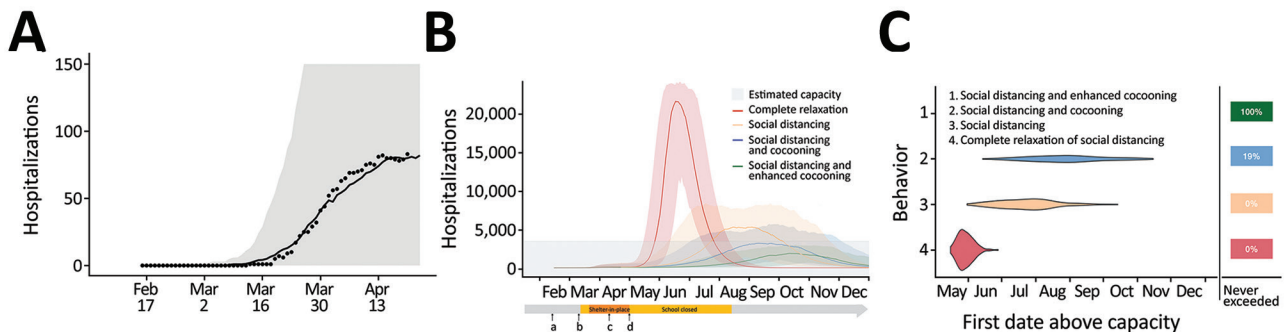


Figure. Projected coronavirus disease (COVID-19) hospitalizations during February 16–December 31, 2020, in the Austin-Round Rock Metropolitan Statistical Area, Texas, USA, assuming strict social distancing measures are relaxed on May 1, 2020. A) To calibrate transmission rates before and after Austin’s March 24 Stay Home–Work Safe Order (order 20200324-007; <https://www.austintexas.gov>), we used least squares to fit our age- and risk-structured susceptible-exposed-infection-recover (SEIR) compartmental model of COVID-19 transmission. Black dots represent daily hospitalization data for the metropolitan area from February 16–April 20, 2020. The curve is the median projection across 200 simulations. Shading represents 95% prediction interval, based on the estimated transmission reduction of 70% beginning March 24. B) Model fitting indicating the ongoing COVID-19 epidemic in Austin. Schools were closed on March 15 and the shelter-in-place order was issued on March 24. a) Date of possible local COVID-19 introduction, February 16; b) date of the first detected case reported, March 13; c) date shelter-in-place order was amended to include cloth face coverings in public, April 13; d) date Texas governor mandated for statewide reopening, May 1. After May 1, we project 4 scenarios in which transmission in low-risk and high-risk groups change relative the reductions achieved during the March 24–May 1 stay-home period: 1) a complete relaxation of measures with transmission rates rebounding to baseline (red); partially relaxed social distancing measures that are 75% as effective as the stay-home order in low-risk groups, with either 2) identical relaxation in high-risk populations (yellow), 3) cocooning that continues to reduce transmission in high-risk groups at the level achieved during the stay-home order (blue), or 4) enhanced cocooning that reduces transmission in high-risk groups further, by 125% relative to the stay home order (green). Lines indicate the median and shading indicates 95% CI across 200 stochastic simulations. Gray shading at bottom indicates 80% of the estimated total daily hospital capacity in the Austin–Round Rock MSA for COVID-19 patients of the 4,299 total beds (3,440). The projections assume that schools open on August 18th. C) The projected first date in 2020 that COVID-19 hospital bed requirements will exceed local capacity for each scenario, as indicated by corresponding colors. The right column indicates the chance that hospitalizations will not exceed capacity in 2020. For example, under enhanced cocooning, we would not expect hospitalizations to exceed capacity.

70% (Appendix Table 1). Postponing relaxation of shelter-in-place measures would not prevent a second pandemic wave but could buy more time to protect vulnerable populations (Appendix Figure 1).

Cities likely will experience additional waves of COVID-19 when social distancing orders are relaxed. Our model indicates that Austin must aggressively reduce SARS-CoV-2 spread to avoid overwhelming hospital capacity by the end of 2020. Without cocooning, measures that reduce transmission with  $\geq 90\%$  the efficacy of the stay-home order are needed; with cocooning, social distancing measures for persons at lower risk can be more relaxed (Appendix Figure 1). Cocooning of older adults and persons with known high-risk conditions (8) can protect thousands in Austin and millions worldwide. The high-risk population in Austin, as in many cities, is diverse; 66% are  $\geq 65$  years of age,  $\approx 5,000$  are residents in LTCs, and almost 3,000 are persons experiencing homelessness (9). Cocooning should be resourced proactively and tailored to meet the distinct needs of high-risk subgroups, including work-at-home and paid leave programs that enable high-risk workers to self-isolate (10). Concerted efforts also are needed to shelter residents of LTCs (3) and persons experiencing homelessness, where risks are compounded by group living conditions that amplify COVID-19 transmission. Thus, cocooning should be added to the national gating criteria prior to relaxation of social distancing.

This article was published as a preprint at <https://www.medrxiv.org/content/10.1101/2020.05.03.20089920v1>.

### Acknowledgments

We thank Matthew Biggerstaff, Michael Johansson, the FluCode network at CDC, Austin Mayor Steven Adler, and the White House Coronavirus Task Force for providing critical discussions and parameter guidance.

### About the Author

Ms. Wang is a PhD candidate at the University of Texas at Austin under the supervision of Dr. Meyers. Her research

interest is in mathematical and statistical modeling of infectious disease dynamics.

### References

1. Mervosh S, Lu D, Swales V. See which states and cities have told residents to stay at home. NY Times. 2020 Apr 20 [cited 2020 Jun 1]. <https://www.nytimes.com/interactive/2020/us/coronavirus-stay-at-home-order.html>
2. White House, Centers for Disease Control and Prevention. Guidelines: opening up America again. Washington: The White House and The Centers; 2020 [cited 2020 Jun 1]. <https://www.whitehouse.gov/wp-content/uploads/2020/04/Guidelines-for-Opening-Up-America-Again.pdf>
3. Centers for Disease Control and Prevention. Coronavirus disease 2019 (COVID-19): performing facility-wide SARS-CoV-2 testing in nursing homes [cited 2020 Jun 1]. <https://www.cdc.gov/coronavirus/2019-ncov/hcp/nursing-homes-facility-wide-testing.html>
4. Centers for Disease Control and Prevention. Coronavirus disease 2019 (COVID-19): CDC COVID data tracker. 2020 Jun 17 [cited 2020 Jun 22]. <https://www.cdc.gov/coronavirus/2019-ncov/cases-updates/cases-in-us.html>
5. Kamp J, Mathews AW. Coronavirus deaths in U.S. nursing, long-term care facilities top 50,000. WSJ Online. 2020 Jun 16 [cited 2020 Jun 16]. <https://www.wsj.com/articles/coronavirus-deaths-in-u-s-nursing-long-term-care-facilities-top-50-000-11592306919>
6. Plohetski T. Coronavirus chronicles: heartache inside Austin, Texas, nursing home. USA Today. 2020 May 8 [cited 2020 Jun 20]. <https://www.usatoday.com/story/news/investigations/2020/05/08/covid-chronicles-heartache-one-u-s-citys-deadliest-nursing-home/3095807001>
7. Wang X, Pasco RF, Du Z, Petty M, Fox SJ, Galvani AP, et al. Impact of social distancing measures on coronavirus disease healthcare demand, central Texas, USA. *Emerg Infect Dis*. 2020 [Epub ahead of print]. <https://doi.org/10.3201/eid2610.201702>
8. US Centers for Disease Control and Prevention. Coronavirus disease 2019 (COVID-19): people with certain medical conditions [cited 2020 Jun 1]. <https://www.cdc.gov/coronavirus/2019-ncov/need-extra-precautions/people-with-medical-conditions.html>
9. ECHO. 2020 Point-in-time count results 2020 May 18 [cited 2020 Jun 20] <https://www.austinecho.org/leading-system-change/data-and-reports/#pit-count-results>
10. US Department of Labor. Temporary rule: paid leave under the families first coronavirus response act [cited 2020 Jun 18]. <https://www.dol.gov/agencies/whd/ffcra>

Address for correspondence: Lauren Ancel Meyers, Department of Integrative Biology; 1 University Station C0990; Austin, TX 78712, USA; email: [laurenmeyers@austin.utexas.edu](mailto:laurenmeyers@austin.utexas.edu)

# Effects of Cocooning on Coronavirus Disease Rates after Relaxing Social Distancing

## Appendix

### Section 1. Appendix Table 1 and Appendix Figure 1

### Section 2. Stochastic Compartmental Model of COVID-19 Transmission in the Austin-Round Rock Metropolitan Statistical Area

The model structure is diagrammed in Appendix Figure 2 and described in the equations below.

For each age and risk group, we built a separate set of compartments to model the transitions between the disease states: susceptible ( $S$ ), exposed ( $E$ ), symptomatic infectious ( $I^Y$ ), asymptomatic infectious ( $I^A$ ), symptomatic infectious that are hospitalized ( $I^H$ ), recovered ( $R$ ), and deceased ( $D$ ). The symbols  $S$ ,  $E$ ,  $I^Y$ ,  $I^A$ ,  $I^H$ ,  $R$ , and  $D$  denote the number of persons in that state in the given age/risk group and the total size of the age/risk group is  $N = S + E + I^Y + I^A + I^H + R + D$ .

The model for persons in age group  $a$  and risk group  $r$  is given by:

$$\begin{aligned} \frac{dS_{a,r}}{dt} &= - \sum_{i \in A} \sum_{j \in K} (I_{i,j}^Y \omega^Y + I_{i,j}^A \omega^A + E_{i,j} \omega^E) \beta \phi_{a,i} / N_i \\ \frac{dE_{a,r}}{dt} &= \sum_{i \in A} \sum_{j \in K} (I_{i,j}^Y \omega^Y + I_{i,j}^A \omega^A + E_{i,j} \omega^E) \beta \phi_{a,i} / N_i - \sigma E_{a,r} \\ \frac{dI_{a,r}^A}{dt} &= (1 - \tau) \sigma E_{a,r} - \gamma^A I_{a,r}^A \\ \frac{dI_{a,r}^Y}{dt} &= \tau \sigma E_{a,r} - (1 - \pi) \gamma^Y I_{a,r}^Y - \pi \eta I_{a,r}^Y \end{aligned}$$

$$\frac{dI_{a,r}^H}{dt} = \pi\eta I_{a,r}^Y - (1 - \nu)\gamma^H I_{a,r}^H - \nu\mu I_{a,r}^H$$

$$\frac{dR_{a,r}}{dt} = \gamma^A I_{a,r}^A + (1 - \pi)\gamma^Y I_{a,r}^Y + (1 - \nu)\gamma^H I_{a,r}^H$$

$$\frac{dD_{a,r}}{dt} = \nu\mu I_{a,r}^H$$

where  $A$  and  $K$  are all possible age and risk groups,  $\omega^A$ ,  $\omega^Y$ , and  $\omega^H$  are relative infectiousness of the  $I^A$ ,  $I^Y$ , and  $E$  compartments, respectively,  $\beta$  is transmission rate,  $\phi_{a,i}$  is the mixing rate between age group  $a$ ,  $i \in A$ ,  $\gamma^A$ ,  $\gamma^Y$ , and  $\gamma^H$  are the recovery rates for the  $I^A$ ,  $I^Y$ , and  $I^H$  compartments, respectively,  $\sigma$  is the exposed rate,  $\tau$  is the symptomatic ratio,  $\pi$  is the proportion of symptomatic persons requiring hospitalization,  $\eta$  is the rate at which hospitalized cases enter the hospital following symptom onset,  $\nu$  is mortality rate for hospitalized cases, and  $\mu$  is rate at which terminal patients die.

We model stochastic transitions between compartments by using the  $\tau$ -leap method (1,2) with key parameters given in Appendix Table 1. Assuming that the events at each time-step are independent and do not affect the underlying transition rates, the numbers of each type of event should follow Poisson distributions with means equal to the rate parameters. We thus simulate the model according to the following equations:

$$S_{a,r}(t+1) - S_{a,r}(t) = -P_1$$

$$E_{a,r}(t+1) - E_{a,r}(t) = P_1 - P_2$$

$$I_{a,r}^A(t+1) - I_{a,r}^A(t) = (1 - \tau)P_2 - P_3$$

$$I_{a,r}^Y(t+1) - I_{a,r}^Y(t) = \tau P_2 - P_4 - P_5$$

$$I_{a,r}^H(t+1) - I_{a,r}^H(t) = P_5 - P_6 - P_7$$

$$R_{a,r}(t+1) - R_{a,r}(t) = P_3 + P_4 + P_6$$

$$D_{a,r}(t+1) - D_{a,r}(t) = P_7,$$

with

$$P_1 \sim \text{Pois}(S_{a,r}(t)F_{a,r}(t))$$

$$P_2 \sim \text{Pois}(\sigma E_{a,r}(t))$$

$$P_3 \sim \text{Pois}(\gamma^A I_{a,r}^A(t))$$

$$P_4 \sim \text{Pois}((1 - \pi)\gamma^Y I_{a,r}^Y(t))$$

$$P_5 \sim \text{Pois}(\pi\eta I_{a,r}^Y(t))$$

$$P_6 \sim \text{Pois}((1 - \nu)\gamma^H I_{a,r}^H(t))$$

$$P_7 \sim \text{Pois}(\nu\mu I_{a,r}^H(t))$$

and where  $F_{a,r}$  denotes the force of infection for persons in age group  $a$  and risk group  $r$  and is given by:

$$F_{a,r}(t) = \sum_{i \in A} \sum_{j \in K} (I_{i,j}^Y(t)\omega^Y + I_{i,j}^A(t)\omega^A + E_{i,j}(t)\omega^E) \beta_{a,i} \phi_{a,i}/N_i.$$

### Parameter Estimation using Austin Hospitalization Data

The city of Austin provided the total number of *heads in beds* for confirmed COVID-19 patients in hospitals in Austin-Round Rock MSA from March 13 to April 24, 2020 (Appendix Table 2). Let  $H(t)$  be the observed and  $\hat{H}(t)$  be the predicted hospitalization totals on day  $t$ , where predictions are made from the deterministic model formulation. We conducted least-squares fitting to estimate  $\beta, \kappa, t_0$ , corresponding to the baseline transmission rate, the reduction in contacts following Austin's Stay Home–Work Safe Order, and the initial seed date of the epidemic respectively.

Fitting was conducted by using the nonlinear least squares method made available in SciPy (3), which minimizes the least squares error defined as  $LSE = (H(t) - \hat{H}(t))^2$  (3). The best fit model accurately captured the hospitalization data and estimated  $\hat{\beta} = 0.035$ ,  $\hat{\kappa} = 0.95$ ,  $\hat{t}_0 =$  February 16, 2020.

We calculated 95% confidence intervals for  $\hat{\kappa}$  by comparing prediction intervals from stochastic simulations with the hospitalization data. We ran 500 stochastic simulations for each of the following possible values of  $\kappa'$ : 0.0, 0.05, ..., 0.95, 1.0. For each value of  $\kappa'$ , we conducted the following analysis to determine if  $\kappa'$  lies inside the 95% confidence interval for  $\kappa'$ .

- For all simulations, we calculate the day-to-day difference in hospitalizations (i.e., *heads in beds*) during the period following the Stay Home–Work Safe order:  $\hat{z}_t = \hat{H}_t - \hat{H}_{t-1}$ . We do the same for the actual data:  $z_t = \overline{H}_t - \overline{H}_{t-1}$ .

- We compute the 95% prediction interval for  $\hat{z}_t$  across all 500 stochastic simulations for  $\kappa'$  for each day  $t$ .
- We then conduct a test of the null hypothesis  $H_0: \kappa' = \kappa$ . Under this null hypothesis, we would expect roughly 95% of the observed data ( $z_t$ ) to fall within the 95% prediction band for  $\hat{z}_t$  that we constructed from our simulations. By analyzing the day-to-day difference in hospitalizations rather than daily hospitalizations, we can assume that the data are independent from one day to the next. Then the expected number of observed values contained in the 95% prediction band is given by the binomial expression:

$$N_{observed} \sim B(N_{points}, 0.95)$$

where  $N_{observed}$  is the number of data points contained within the 95% prediction band and  $N_{points}$  is the total number of data points (i.e., days).

- We calculate  $N_{contained}$ , the actual number of data points contained within the 95% prediction band, and compute a p-value by identifying the probability that one would observe  $N_{contained}$  or more extreme results under the null distribution. If  $p < 0.05$ , we reject the null hypothesis  $H_0: \kappa' = \kappa$ .

### **Model Parameters**

Model parameters are provided in Appendix Tables 3–9.

## **Section 3. Sensitivity Analyses**

### **Sensitivity Analysis with Respect to Age-Specific Contact Rates**

We conducted a sensitivity analysis in which we modeled the same 4 scenarios but without any age-specific contact rates. That is, we removed the contact matrices altogether and assume that transmission rates are homogeneous across the population. Under these conditions, we would expect cocooning to have an even larger beneficial effect (Appendix Figure 3). Specifically, 9% of the 200 simulations exceed hospital capacity with cocooning assuming homogeneous contact rates, where the number is 19% with contact matrices. The reduction in peak hospitalization with cocooning is also higher when assuming homogeneous mixing. This likely stems from our primary model (with contact matrices) assuming that persons  $\geq 65$  years of

age have fewer contacts on average than younger adults and children. In a sense, they are naturally cocooned by their baseline behavior. In the homogeneous contact model, this large high-risk group is more exposed, and thus even moderate cocooning has a large protective effect.

#### **Sensitivity Analysis with Respect to Cocooning of High-Risk Persons <65 Years of Age**

In the cocooned population, 34% are  $\geq 65$  years of age and 66% are younger persons with  $\geq 1$  chronic condition, as described in Appendix Section 4. When we restrict cocooning in our model to protect only persons  $\geq 65$  years of age, the projected epidemiologic effects are reduced (Appendix Figure 4). Not only does this reduce protection to only 34% of the vulnerable population, but it targets the subset of the high-risk population with the lowest contact rates. The younger high-risk populations who remain exposed are more likely to become infected and infect others because of their higher rates of daily contacts.

### **Section 4. Estimation of Age-Stratified Proportion of Population at High Risk for COVID-19 Complications**

We estimated age-specific proportions of the population at high risk for complications from COVID-19 based on data for Austin, TX and Round-Rock, TX from the 500 Cities Project by the US Centers for Disease Control and Prevention (CDC) (16; Appendix Figure 5).

We assumed that high-risk conditions for COVID-19 are the same as those specified for influenza by the CDC (10). The CDC's 500 Cities Project provides city-specific estimates of prevalence for several of these conditions among adults (23). The estimates were obtained from the 2015–2016 Behavioral Risk Factor Surveillance System (BRFSS, <https://www.cdc.gov/brfss/index.html>) data by using a small-area estimation methodology called multilevel regression and poststratification (11,12), which links geocoded health surveys to high spatial resolution population demographic and socioeconomic data (12).

#### **Estimating High-Risk Proportions for Adults**

To estimate the proportion of adults at high risk for complications, we used CDC's 500 cities data, as well as data on the prevalence of HIV/AIDS, obesity, and pregnancy among adults (Appendix Table 10).

The CDC 500 cities dataset includes the prevalence of each condition on its own, rather than the prevalence of multiple conditions (e.g., dyads or triads). Thus, we use separate

comorbidity estimates to determine overlap. Reference about chronic conditions (24) gives United States estimates for the proportion of the adult population with 0, 1, or  $\geq 2$  chronic conditions, per age group. By using this and the 500 cities data we can estimate the proportion of the population (pHR) in each age group in each city with  $\geq 1$  chronic condition listed in the CDC 500 cities data (Appendix Table 10) putting them at high-risk for complications from influenza.

#### **HIV**

We used the data from Table 20a in CDC HIV surveillance report (17) to estimate the population in each risk group living with HIV in the United States (last column, 2015 data). Assuming independence between HIV and other chronic conditions, we increased the proportion of the population at high risk for influenza to account for persons with HIV but no other underlying conditions.

#### **Morbid Obesity**

A body mass index (BMI)  $>40$  kg/m<sup>2</sup> indicates morbid obesity and is considered high risk for influenza. The 500 Cities Project reports the prevalence of obese persons in each city with BMI  $>30$  kg/m<sup>2</sup> (not necessarily morbid obesity). We use the data from Table 1 in Sturm and Hattori (18) to estimate the proportion of persons with BMI  $>30$  kg/m<sup>2</sup> that actually have BMI  $>40$  kg/m<sup>2</sup> across the United States; we then apply this to the 500 cities obesity data to estimate the proportion of persons who are morbidly obese in each city. Table 1 of Morgan et al. (19) suggests that 51.2% of morbidly obese adults have  $\geq 1$  other high-risk chronic condition, and update our high-risk population estimates accordingly to account for overlap.

#### **Pregnancy**

We separately estimated the number of pregnant women in each age group and each city, following the methodology in CDC reproductive health report (25). We assume independence between any of the high-risk factors and pregnancy and further assume that half the population are women.

#### **Estimating High-Risk Proportions for Children**

Since the 500 Cities Project only reports data for adults  $\geq 18$  years of age, we took a different approach to estimating the proportion of children at high risk for severe influenza. The 2 most prevalent risk factors for children are asthma and obesity; we also accounted for childhood diabetes, HIV, and cancer.

From Miller et al. (26), we obtained national estimates of chronic conditions in children. For asthma, we assumed that variation among cities would be similar for children and adults. Thus, we used the relative prevalence of asthma in adults to scale our estimates for children in each city. The prevalence of HIV and cancer in children are taken from CDC HIV surveillance report (18) and cancer research report (27).

We first estimated the proportion of children having either asthma, diabetes, cancer, or HIV, assuming no overlap in these conditions. We estimated city-level morbid obesity in children by using the estimated morbid obesity in adults multiplied by a national constant ratio for each age group estimated from Hales et al. (28) that represents the prevalence in morbid obesity in children given the prevalence observed in adults. From Morgan et al. (19), we estimated that 25% of morbidly obese children have another high-risk condition and adjusted our final estimates accordingly.

## Resulting Estimates

We compared our estimates for the Austin-Round Rock MSA to published national-level estimates (29) of the proportion of each age group with underlying high-risk conditions (Appendix Table 11). The biggest difference was observed in older adults, with Austin having a lower proportion at risk for complications from COVID-19 than the national average; for persons 25–39 years of age, the high-risk proportion was slightly higher than the national average (Appendix Figure 5).

## References

1. Keeling MJ, Rohani P. Modeling infectious diseases in humans and animals. Princeton (MA): Princeton University Press; 2011.
2. Gillespie DT. Approximate accelerated stochastic simulation of chemically reacting systems. *J Chem Phys.* 2001;115:1716–33. <https://doi.org/10.1063/1.1378322>
3. The SciPy Community. `scipy.optimize.least_squares`—SciPy v1.4.1 reference guide. [cited 2020 Apr 26]. [https://docs.scipy.org/doc/scipy/reference/generated/scipy.optimize.least\\_squares.html](https://docs.scipy.org/doc/scipy/reference/generated/scipy.optimize.least_squares.html)

4. Prem K, Cook AR, Jit M. Projecting social contact matrices in 152 countries using contact surveys and demographic data. *PLoS Comput Biol*. 2017;13:e1005697. [PubMed](#)  
<https://doi.org/10.1371/journal.pcbi.1005697>
5. Mossong J, Hens N, Jit M, Beutels P, Auranen K, Mikolajczyk R, et al. Social contacts and mixing patterns relevant to the spread of infectious diseases. *PLoS Med*. 2008;5:e74. [PubMed](#)  
<https://doi.org/10.1371/journal.pmed.0050074>
6. He X, Lau EHY, Wu P, Deng X, Wang J, Hao X, et al. Temporal dynamics in viral shedding and transmissibility of COVID-19. *Nat Med*. 2020;26:672–5 [PubMed](#).  
<https://doi.org/10.1038/s41591-020-0869-5>
7. Gudbjartsson DF, Helgason A, Jonsson H, Magnusson OT, Melsted P, Norddahl GL, et al. Spread of SARS-CoV-2 in the Icelandic Population. *N Engl J Med*. 2020;382:2302–15. [PubMed](#)  
<https://doi.org/10.1056/NEJMoa2006100>
8. Zhang J, Litvinova M, Wang W, Wang Y, Deng X, Chen X, et al. Evolving epidemiology and transmission dynamics of coronavirus disease 2019 outside Hubei province, China: a descriptive and modelling study. *Lancet Infect Dis*. 2020;20:793–802. [PubMed](#)  
[https://doi.org/10.1016/S1473-3099\(20\)30230-9](https://doi.org/10.1016/S1473-3099(20)30230-9)
9. Verity R, Okell LC, Dorigatti I, Winskill P, Whittaker C, Imai N, et al. Estimates of the severity of coronavirus disease 2019: a model-based analysis. *Lancet Infect Dis*. 2020;20:669–77. [PubMed](#)  
[https://doi.org/10.1016/S1473-3099\(20\)30243-7](https://doi.org/10.1016/S1473-3099(20)30243-7)
10. US Centers for Disease Control and Prevention. People at high risk for flu complications. 2019 [cited 2020 Mar 26]. <https://www.cdc.gov/flu/highrisk>
11. US Centers for Disease Control and Prevention. Behavioral Risk Factor Surveillance System (BRFSS). 2019 [cited 2020 Jun 22]. <https://www.cdc.gov/brfss>
12. Zhang X, Holt JB, Lu H, Wheaton AG, Ford ES, Greenlund KJ, et al. Multilevel regression and poststratification for small-area estimation of population health outcomes: a case study of chronic obstructive pulmonary disease prevalence using the behavioral risk factor surveillance system. *Am J Epidemiol*. 2014;179:1025–33. [PubMed](#) <https://doi.org/10.1093/aje/kwu018>
13. Stokes EK, Zambrano LD, Anderson KN, Marder EP, Raz KM, El Burai Felix S, et al. Coronavirus disease 2019 case surveillance—United States, January 22–May 30, 2020. *MMWR Morb Mortal Wkly Rep*. 2020;69:759–65. [PubMed](#) <https://doi.org/10.15585/mmwr.mm6924e2>

14. Austin Independent School District. Calendar of events [cited 2020 Mar 26].  
<https://www.austinisd.org/calendar>
15. Tindale L, Coombe M, Stockdale JE, Garlock E, Lau WYV, Saraswat M, et al. Transmission interval estimates suggest pre-symptomatic spread of COVID-19. *eLife*. 2020;9:e57149. [PubMed](#)  
<https://doi.org/10.7554/eLife.57149>
16. US Centers for Disease Control and Prevention. 500 Cities project: local data for better health. 2019 [cited 2020 Jun 22]. <https://www.cdc.gov/500cities>
17. US Centers for Disease Control and Prevention. HIV surveillance report, 2016 [cited 2020 Jun 1].  
<http://www.cdc.gov/hiv/library/reports/hiv-surveillance.html>
18. Sturm R, Hattori A. Morbid obesity rates continue to rise rapidly in the United States. *Int J Obes*. 2013;37:889–91. [PubMed](#) <https://doi.org/10.1038/ijo.2012.159>
19. Morgan OW, Bramley A, Fowlkes A, Freedman DS, Taylor TH, Gargiullo P, et al. Morbid obesity as a risk factor for hospitalization and death due to 2009 pandemic influenza A(H1N1) disease. *PLoS One*. 2010;5:e9694. [PubMed](#) <https://doi.org/10.1371/journal.pone.0009694>
20. Martin JA, Hamilton BE, Osterman MJK, Driscoll AK, Drake P. Births: final data for 2017. *Natl Vital Stat Rep*. 2018;67:1–50 [PubMed](#)
21. Jatlaoui TC, Boutot ME, Mandel MG, Whiteman MK, Ti A, Petersen E, et al. Abortion surveillance—United States, 2015. *MMWR Surveill Summ*. 2018;67:1–45. [PubMed](#)  
<https://doi.org/10.15585/mmwr.ss6713a1>
22. Ventura SJ, Curtin SC, Abma JC, Henshaw SK. Estimated pregnancy rates and rates of pregnancy outcomes for the United States, 1990–2008. *Natl Vital Stat Rep*. 2012;60:1–21. [PubMed](#)
23. US Centers for Disease Control and Prevention. 500 Cities project: health outcomes. 2019 [cited 2020 Jun 22]. <https://www.cdc.gov/500cities/definitions/health-outcomes.htm>
24. Fox S, Duggan M. Pew Research Center. The diagnosis difference. Part one: who lives with chronic conditions. 2013 [cited 2020 Jun 22]. <https://www.pewresearch.org/internet/2013/11/26/part-one-who-lives-with-chronic-conditions>
25. US Centers for Disease Control and Prevention. Estimating the number of pregnant women in a geographic area [cited 2020 Jun 1].  
<https://www.cdc.gov/reproductivehealth/emergency/pdfs/PregnacyEstimatoBrochure508.pdf>

26. Miller GF, Coffield E, Leroy Z, Wallin R. Prevalence and costs of five chronic conditions in children. *J Sch Nurs.* 2016;32:357–64. [PubMed https://doi.org/10.1177/1059840516641190](https://doi.org/10.1177/1059840516641190)
27. American Cancer Society. Cancer facts and figures 2014 [cited 2020 Jun 22]. <https://www.cancer.org/research/cancer-facts-statistics/all-cancer-facts-figures/cancer-facts-figures-2014.html>
28. Hales CM, Fryar CD, Carroll MD, Freedman DS, Ogden CL. Trends in obesity and severe obesity prevalence in US youth and adults by sex and age, 2007–2008 to 2015–2016. *JAMA.* 2018;319:1723–5. [PubMed https://doi.org/10.1001/jama.2018.3060](https://doi.org/10.1001/jama.2018.3060)
29. Zimmerman RK, Lauderdale DS, Tan SM, Wagener DK. Prevalence of high-risk indications for influenza vaccine varies by age, race, and income. *Vaccine.* 2010;28:6470–7. [PubMed https://doi.org/10.1016/j.vaccine.2010.07.037](https://doi.org/10.1016/j.vaccine.2010.07.037)

**Appendix Table 1.** Estimated time until coronavirus disease hospitalizations exceed local hospital bed surge capacity during February 16–December 31, 2020 based on effectiveness of various public health measures, Austin-Round Rock metropolitan statistical area, Texas, USA\*

Measures	% Effectiveness†				
	0	50	75	90	95
<b>No cocooning</b>					
No. days to exceed surge capacity	27 (16–43)	44 (26–77)	84 (41–137)	NE (133–NE)	NE
Cumulative no. hospital beds	82,146 (79,331–84,276)	68,403 (62,593–72,733)	52,452 (45,748–59,083)	31,018 (5,332–41,805)	14,247 (505–33,329)
Cumulative no. deaths	10,139 (9,598–10,509)	8,046 (7,143–8,703)	5,822 (4,939–6,791)	3,192 (437–4,501)	1,340 (44–3,510)
<b>Cocooning</b>					
No. days to exceed surge capacity	38 (25–58)	62 (38–114)	127 (63–NE)	NE	NE
Cumulative no. hospital beds	49,637 (45,173–53,119)	44,447 (38,490–49,568)	37,449 (27,611–43,685)	21,411 (1,625–33,957)	9,905 (336–27,609)
Cumulative no. deaths	5,156 (4,535–5,611)	4,622 (3,886–5,290)	3,857 (2,714–4,618)	2,076 (141–3,505)	894 (32–2,740)
<b>Enhanced cocooning</b>					
Days to exceed surge capacity	47 (34–68)	87 (57–173)	NE	NE	NE
Cumulative hospital beds	30,778 (28,133–33,544)	26,407 (23,355–29,384)	19,927 (10,070–24,641)	3,371 (35–13,771)	838 (56–7,075)
Cumulative deaths	2,745 (2,473–3,048)	2,362 (2,056–2,698)	1,755 (770–2,276)	260 (2–1,187)	77 (5–613)

\*Assuming that social distancing measures are relaxed on May 1, 2020. Values are expressed as median (95% CI) across 200 stochastic simulations based on the parameters given in Appendix. NE, not expected to surpass the specified thresholds before December 31, 2020.

†Compared with Stay Home–Work Safe order.

**Appendix Table 2.** Number of persons hospitalized for coronavirus disease each day during March 13–April 24, 2020, Austin-Round Rock metropolitan area, Texas, USA

Date	No. persons hospitalized
13 Mar 2020	1
14 Mar 2020	1
15 Mar 2020	1
16 Mar 2020	1
17 Mar 2020	1
18 Mar 2020	1
19 Mar 2020	5
20 Mar 2020	7
21 Mar 2020	6
22 Mar 2020	9
23 Mar 2020	10
24 Mar 2020	17
25 Mar 2020	22
26 Mar 2020	25
27 Mar 2020	25
28 Mar 2020	29
29 Mar 2020	32
30 Mar 2020	41
31 Mar 2020	44
1 Apr 2020	52
2 Apr 2020	56
3 Apr 2020	57
4 Apr 2020	63
5 Apr 2020	65
6 Apr 2020	69
7 Apr 2020	69
8 Apr 2020	70
9 Apr 2020	71
10 Apr 2020	75
11 Apr 2020	76
12 Apr 2020	75
13 Apr 2020	81
14 Apr 2020	82
15 Apr 2020	80
16 Apr 2020	80
17 Apr 2020	79
18 Apr 2020	78
19 Apr 2020	79
20 Apr 2020	83
21 Apr 2020	78
22 Apr 2020	82
23 Apr 2020	78
24 Apr 2020	75

**Appendix Table 3.** Initial conditions, school closures, and social distancing policies for coronavirus disease during 2020 in the Austin-Round Rock metropolitan statistical area, Texas, USA

Variable	Settings
Initial day of simulation	16 Feb 2020
Initial infection number in locations	1 symptomatic case in 18–49 y age group
School closures	15 Mar–17 Aug 2020
Age-specific and day-specific contact rates*	Home, work, other and school matrices provided in Appendix Tables 6–9
During 16 Feb–18 Mar	
Weekday	Home + school + work + other
Weekend	Home + other
Weekday holiday	Home + other
During 19–24 Mar	
Weekday	Home + work + other
Weekend	Home + other
Weekday holiday	Home + other
During 25 Mar–17 Aug	
Weekday	$(1 - \kappa) \times (\text{home} + \text{work} + \text{other})$
Weekend	$(1 - \kappa) \times (\text{home} + \text{other})$
Weekday holiday	$(1 - \kappa) \times (\text{home} + \text{other})$
During 18 Aug–Dec 31	
Weekday	$(1 - \kappa) \times (\text{home} + \text{school} + \text{work} + \text{other})$
Weekend	$(1 - \kappa) \times (\text{home} + \text{other})$
Weekday holiday	$(1 - \kappa) \times (\text{home} + \text{other})$

\*We assume the age-specific contact rates given in (4), which takes the contact numbers estimated through diary-based POLYMOD study in Europe (5) and extrapolates to the United States. The values in Appendix Tables 6–9 are the assumed daily contacts between each pair of age groups at home, school, work, and all other places, respectively. For example, the value of 2.0 in Table A6 row 1 column 2 means that 1 person in the 0–4 age group is estimated to contact 2 people daily in the 18–64 age group at home. These contact matrices are used to adjust the transmission rate between age groups. The accuracy of the contact matrices is limited by the following: possible biases with the original diary-based study (5); assumptions made when projecting the original study to the United States (4); and impacts of coronavirus disease policies and perceptions on daily contact patterns.

**Appendix Table 4.** Model parameters\*

Parameters	Values	Source
$R_0$ , basic reproduction number	2.8	Derived from fitted model
$\delta$ , doubling time before intervention, d	2.9	Derived from fitted model
$\beta$ , baseline transmission rate	0.057	Fitted to daily COVID-19 hospitalizations in Austin-Round Rock MSA, Texas
$\kappa$ , reduction in transmission		During 25 Mar–1 May 2020, fitted to daily COVID-19 hospitalizations in Austin-Round Rock MSA, Texas
15 Feb–24 Mar 2020	0	
25 Mar–1 May 2020	0.7 (95% CI 0.7–1)	
25 Mar–31 Dec 2020		
Scenario 1	0	
Scenario 2	0.5	
Scenario 3	0.7	
Scenario 4	0.9	
Scenario 5	0.95	
$c$ , cocooning efficacy; the reduction in transmission relative to Austin’s Stay Home–Work Safe Order for all high-risk groups		Assumption
Cocooning	1.0	
Enhanced cocooning	1.25	
$\gamma^A$ , recovery rate on asymptomatic compartment	Equal to $\gamma^Y$	
$\gamma^Y$ , recovery rate on symptomatic nontreated compartment	$\frac{1}{\gamma^Y} \sim \text{Triangular}$ (5.3, 6.3, 7.3)	(6)
$\tau$ , symptomatic proportion, %	$\approx \gamma$ 57	(7)
$\sigma$ , exposed rate†	$\frac{1}{\sigma} \sim \text{Triangular}$ (1.9, 2.9, 3.9)	(6,8)
$\omega^A$ , relative infectiousness of infectious persons in compartment $I^A$	$\approx \sigma$ 0.67	(6)
IFR, infected fatality ratio, age specific, %		Age adjusted from R. Verity et al. (9)
Low-risk group		
0–4 y	0.0009	
5–17 y	0.0022	
18–49 y	0.0339	
50–64 y	0.2520	

Parameters	Values	Source
≥65 y	0.6440	
High-risk group		
0–4 y	0.0092	
5–17 y	0.0218	
18–49 y	0.3388	
50–64 y	2.5197	
≥65 y	6.4402	
YFR, symptomatic fatality ratio, age-specific, %		$YFR = \frac{IFR}{R}$
Low-risk group		
0–4 y	0.0011165	
5–17 y	0.0027	
18–49 y	0.0412	
50–64 y	0.3069	
≥65 y	0.7844	
High-risk group		
0–4 y	0.0112	
5–17 y	0.0265	
18–49 y	0.4126	
50–64 y	3.0690	
≥65 y	7.8443	
<i>h</i> , high-risk proportion, age-specific, %		(10–12)‡
0–4 y	8.2825	
5–17 y	14.1121	
18–49 y	16.5298	
50–64 y	32.9912	
≥65 y	47.0568	
<i>rr</i> , relative risk for high-risk compared with low-risk persons in an age group	10	(13)
School calendars	Austin Independent School District calendar (2019–20, 2020–21)	(14)

\*CDC, US Centers for Disease Control and Prevention; COVID-19, coronavirus disease; MSA, metropolitan statistical area.

†Based on incubation (8) and presymptomatic periods (6).

‡Estimated using 2015–2016 Behavioral Risk Factor Surveillance System (BRFSS; <https://www.cdc.gov/brfss/index.html>) data with multilevel regression and poststratification by using US Centers for Disease Control and Prevention’s list of conditions that may increase the risk for serious complications from influenza.

#### Appendix Table 5. Hospitalization parameters

Parameters	Values	Source
$\gamma^H$ : recovery rate in hospitalized compartment	1/14	14 d-average from admission to discharge (UT Austin Dell Med)
YHR: symptomatic case hospitalization rate (%)		Age adjusted from R. Verity et al. (9)
Low-risk group		
0–4 y	0.0279	
5–17 y	0.0215	
18–49 y	1.3215	
50–64 y	2.8563	
≥65 y	3.3873	
High-risk group		
0–4 y	0.2791	
5–17 y	0.2146	
18–49 y	13.2154	
50–64 y	28.5634	
≥65 y	33.8733	
$\pi$ , rate of symptomatic individuals go to hospital, age-specific	$\pi = \frac{\gamma^Y \times YHR}{\eta + (\gamma^Y - \eta)YHR}$	
$\eta$ , rate from symptom onset to hospitalized	0.1695	5.9-day average from symptom onset to hospital admission Tindale et al. (15)
$\mu$ , rate from hospitalized to death	1/14	14-day average from admission to death (UT Austin Dell Med)
HFR, hospitalized fatality ratio, age-specific, %		$HFR = \frac{IFR}{YHR(1 - \tau)}$

Parameters	Values	Source
0–4 y	4	$V = \frac{j^{HFR}}{\mu + (j^H - \mu)HFR}$
5–17 y	12.365	
18–49 y	3.122	
50–64 y	10.745	
≥65 y	23.158	
$\nu$ , death rate on hospitalized persons, age-specific		
0–4 y	0.0390	
5–17 y	0.1208	
18–49 y	0.0304	
50–64 y	0.1049	
≥65 y	0.2269	
Healthcare capacity, no. hospital beds	4,299	Estimates provided by each of the region's hospital systems and aggregated by regional public health leaders

**Appendix Table 6.** Home contact matrix (daily number contacts by age group at home)

Age, y	0–4	5–17	18–49	50–64	≥65
0–4	0.5	0.9	2.0	0.1	0.0
5–17	0.2	1.7	1.9	0.2	0.0
18–49	0.2	0.9	1.7	0.2	0.0
50–64	0.2	0.7	1.2	1.0	0.1
≥65	0.1	0.7	1.0	0.3	0.6

**Appendix Table 7.** School contact matrix (daily number contacts by age group at school)

Age, y	0–4	5–17	18–49	50–64	≥65
0–4	1.0	0.5	0.4	0.1	0.0
5–17	0.2	3.7	0.9	0.1	0.0
18–49	0.0	0.7	0.8	0.0	0.0
50–64	0.1	0.8	0.5	0.1	0.0
≥65	0.0	0.0	0.1	0.0	0.0

**Appendix Table 8.** Work contact matrix (daily number contacts by age group at work)

Age, y	0–4	5–17	18–49	50–64	≥65
0–4	0.0	0.0	0.0	0.0	0.0
5–17	0.0	0.1	0.4	0.0	0.0
18–49	0.0	0.2	4.5	0.8	0.0
50–64	0.0	0.1	2.8	0.9	0.0
≥65	0.0	0.0	0.1	0.0	0.0

**Appendix Table 9.** Others contact matrix (daily number contacts by age group at other locations)

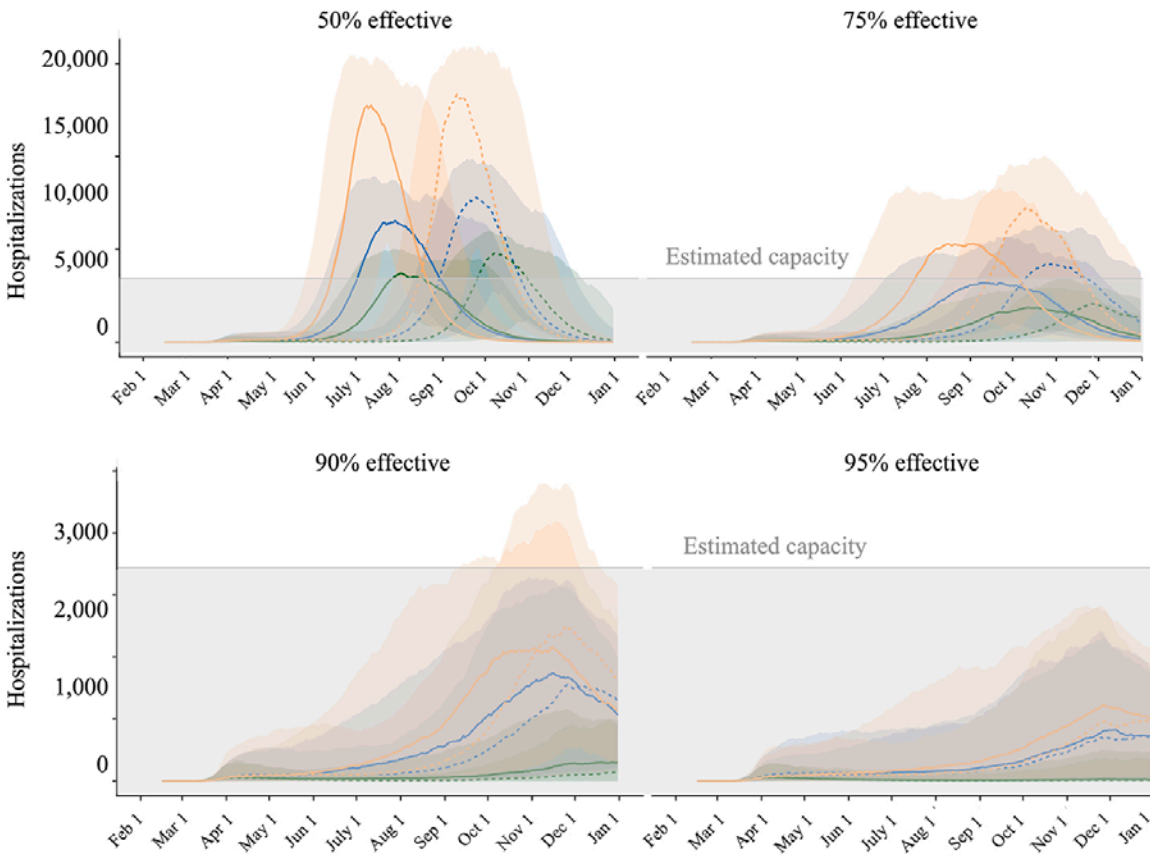
Age, y	0–4	5–17	18–49	50–64	≥65
0–4	0.7	0.7	1.8	0.6	0.3
5–17	0.2	2.6	2.1	0.4	0.2
18–49	0.1	0.7	3.3	0.6	0.2
50–64	0.1	0.3	2.2	1.1	0.4
≥65	0.0	0.2	1.3	0.8	0.6

**Appendix Table 10.** Underlying conditions that put persons at high risk for influenza and data sources for prevalence estimation used in this model

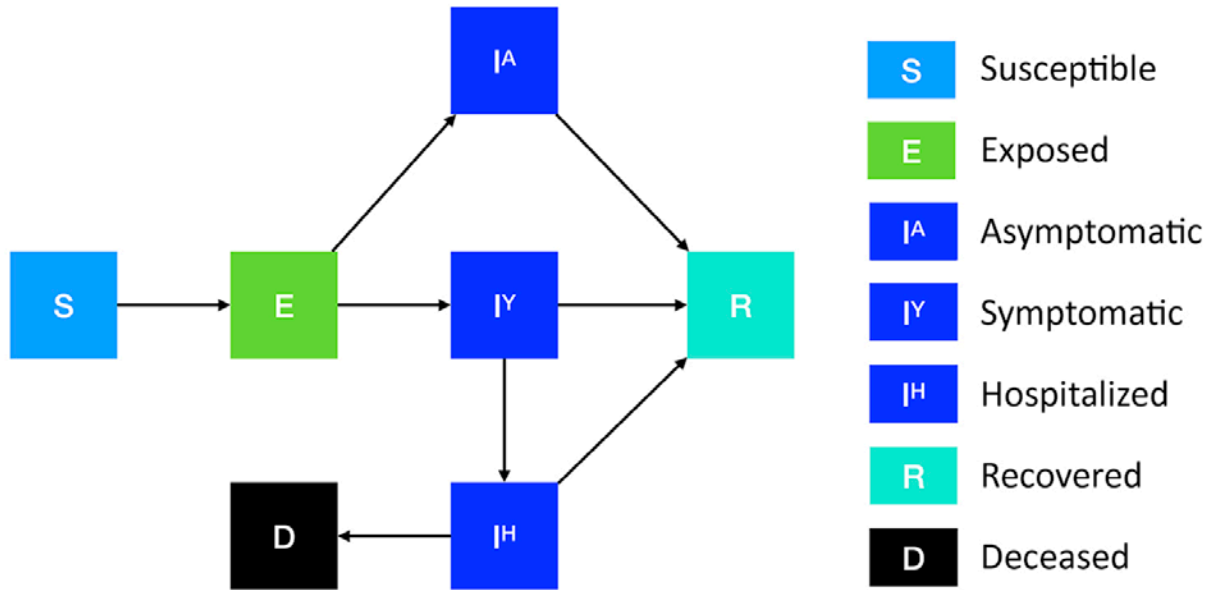
Condition	Data source
Cancer (except skin), chronic kidney disease, COPD, coronary heart disease, stroke, asthma, diabetes	US Centers for Disease Control and Prevention (CDC) 500 cities (16)
HIV/AIDS	CDC HIV Surveillance report (17)
Obesity	CDC 500 cities (16); Sturm and Hattori (18); Morgan et al. (19)
Pregnancy	National Vital Statistics Reports (20) and abortion data (21)

**Appendix Table 11.** Comparison between published national estimates of the percentage of the population at high risk for complications of influenza or coronavirus disease and the percentage of population of Austin-Round Rock metropolitan statistical, Texas, USA

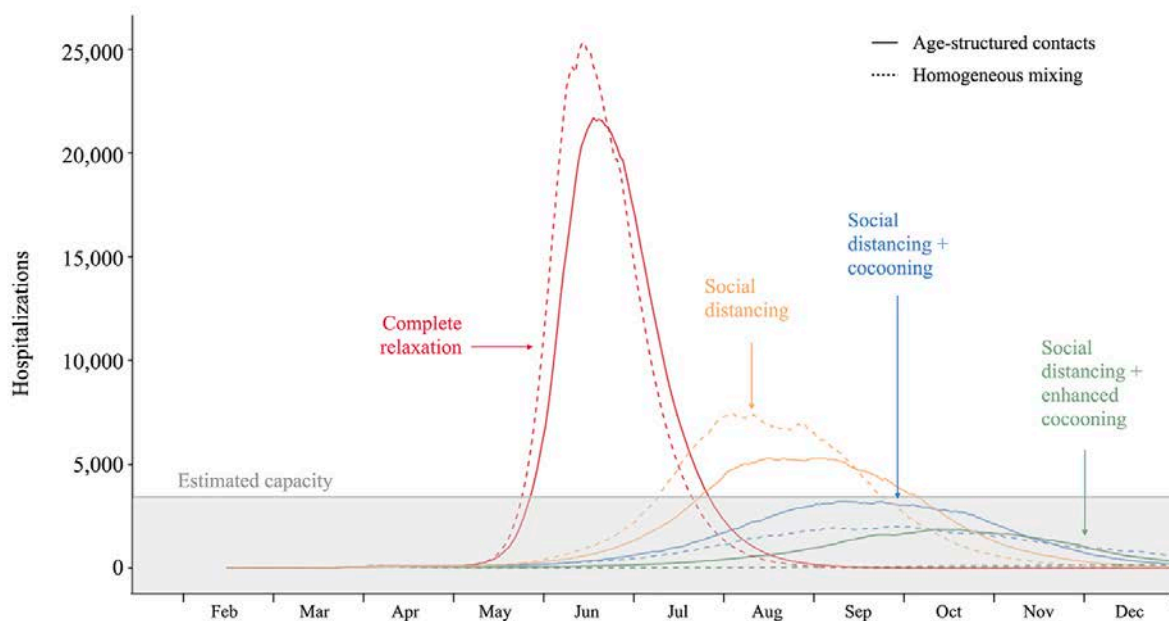
Age group	National estimates (27)	Austin (excluding pregnancy)	Pregnant women (proportion of age group)
0-<6 mo	NA	6.8	–
6 mo–4 y	6.8	7.4	–
5–9 y	11.7	11.6	–
10–14 y	11.7	13.0	–
15–19 y	11.8	13.3	1.7
20–24 y	12.4	10.3	5.1
25–34 y	15.7	13.5	7.8
35–39 y	15.7	17.0	5.1
40–44 y	15.7	17.4	1.2
45–49 y	15.7	17.7	–
50–54 y	30.6	29.6	–
55–59 y	30.6	29.5	–
60–64 y	30.6	29.3	–
65–69 y	47.0	42.2	–
70–74 y	47.0	42.2	–
>75 y	47.0	42.2	–



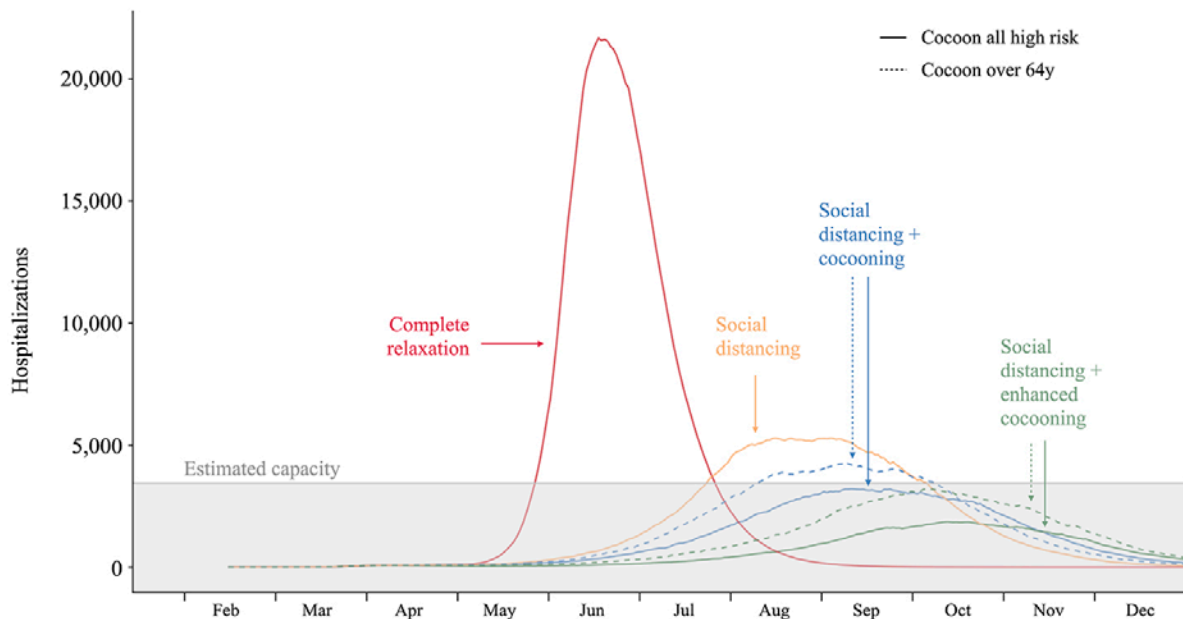
**Appendix Figure 1.** Projected daily coronavirus disease (COVID-19) hospitalizations during February 16–December 31, 2020 in the Austin-Round Rock metropolitan statistical area with different degrees of transmission reduction after the relaxation of the Stay Home–Work Safe order. Solid lines indicate relaxation of Stay Home–Work Safe order on May 1. Dashed lines indicate relaxation of the order on July 1. Before May 1, we estimated that social distancing reduced COVID-19 transmission by 70% relative to the baseline before school closures in Austin on March 15. After May 1, we considered relaxation of the stay-home orders for low-risk groups as scenarios in which transmission was only 50% (top left), 75% (top right), 90% (bottom left), and 95% (bottom right) as effective as during the Stay Home–Work Safe order. Blue lines assume cocooning of vulnerable populations; that is, everyone  $\geq 65$  years of age and persons with high-risk underlying conditions continue to social distance and take precautions that reduce their infection risk the same level as the 70% stay-home order. Green lines assume enhanced cocooning that is 125% as effective as the stay-home order. The yellow lines project COVID-19 cases assuming vulnerable populations have the same transmission reduction as the rest of the population. Lines and shading indicate the median and 95% prediction interval across 200 stochastic simulations.



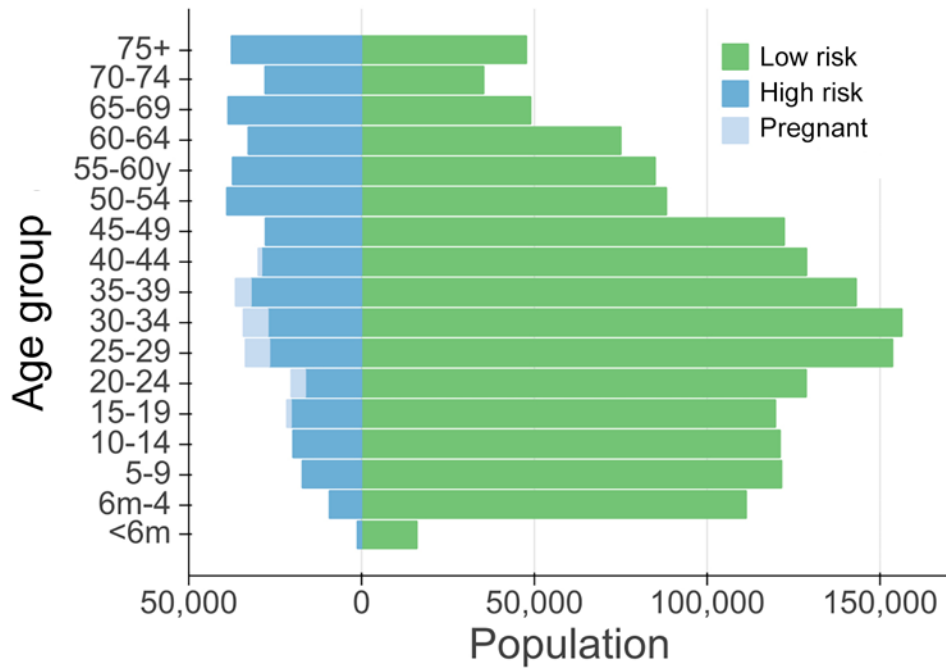
**Appendix Figure 2.** Compartmental model of coronavirus disease (COVID-19) transmission in a US city. Each subgroup (defined by age and risk) is modeled with a separate set of compartments. Upon infection, susceptible individuals ( $S$ ) progress to exposed ( $E$ ) and then to either symptomatic infectious ( $I^Y$ ) or asymptomatic infectious ( $I^A$ ). All asymptomatic cases eventually progress to a recovered class where they remain protected from future infection ( $R$ ); symptomatic cases are either hospitalized ( $I^H$ ) or recover. Mortality ( $D$ ) varies by age group and risk group and is assumed to be preceded by hospitalization.



**Appendix Figure 3.** Sensitivity analysis of hospitalizations in the Austin-Round Rock MSA from February 16 to December 31, 2020 assuming strict social distancing measures are relaxed on May 1, 2020. Solid lines indicate original age-structured contact rates; dashed lines indicate homogeneous mixing. Curves indicate median projections of COVID-19 hospitalizations. The model fitting indicates that the ongoing COVID-19 epidemic in Austin was seeded by a local case around February 16, 2020; the first detected case was reported on March 13, 2020, schools were closed on March 15, and the shelter-in-place order was issued on March 24 and then amended to require cloth face coverings in public on April 13, 2020; the Texas governor mandated statewide reopening beginning May 1. We estimate that transmission was reduced by 70% under the original model (solid) and 75% under the homogeneous model (dashed) beginning March 24th. Following the May 1, we project four scenarios in which transmission in low risk and high risk groups change relative the reductions achieved during the March 24–May 1 stay-home period: (i) a complete relaxation of measures with transmission rates rebounding to baseline (red lines); partially relaxed social distancing measures that are 75% as effective as the stay-home order in low risk groups, with either (ii) identical relaxation in high risk populations (yellow lines), (iii) cocooning that continues to reduce transmission in high risk groups at the level achieved during the stay-home order (blue lines), or (iv) enhanced cocooning that reduces transmission in high risk groups further, by 125% relative to the stay home order (green lines).



**Appendix Figure 4.** Sensitivity analysis of hospitalizations in the Austin-Round Rock MSA from February 16–December 31, 2020 assuming strict social distancing measures are relaxed on May 1, 2020. Solid lines indicate cocooning of all high-risk persons; dashed lines indicate cocooning only persons  $\geq 65$  years of age. Curves indicate median projections of COVID-19 hospitalizations. The model fitting indicates that the ongoing COVID-19 epidemic in Austin was seeded by a local case around February 16, 2020; the first detected case was reported on March 13, 2020, schools were closed on March 15, and the shelter-in-place order was issued on March 24 and then amended to require cloth face coverings in public on April 13, 2020; the Texas governor mandated statewide reopening beginning May 1. We estimate that transmission was reduced by 70% beginning March 24. Following May 1, we project 4 scenarios in which transmission in low-risk and high-risk groups changes relative to reductions achieved during the March 24–May 1 stay-home period: (i) a complete relaxation of measures with transmission rates rebounding to baseline (red lines); partially relaxed social distancing measures that are 75% as effective as the stay-home order in low risk groups, with either (ii) identical relaxation in high risk populations (yellow lines) or (iii) cocooning that continues to reduce transmission in high risk groups at the level achieved during the stay-home order (blue lines); or (iv) enhanced cocooning that reduces transmission in high risk groups further, by 125% relative to the stay home order (green lines).



**Appendix Figure 5.** Demographic and risk composition of the Austin-Round Rock population. Bars indicate age-specific population sizes, separated by low-risk, high-risk, and pregnant persons. High-risk persons are defined as persons with cancer, chronic kidney disease, chronic obstructive pulmonary disease, heart disease, stroke, asthma, diabetes, HIV/AIDS, or morbid obesity, as estimated from the CDC 500 Cities Project (16), reported HIV prevalence (17), and reported morbid obesity prevalence (18,19), corrected for multiple conditions. The population of pregnant women is derived by using CDC’s method combining fertility, abortion, and fetal loss rates (20–22).